Appl Microbiol Biotechnol (2012) 93:83–93
DOI 10.1007/s00253-011-3682-8

MINI-REVIEW

L-Proline dehydrogenases in hyperthermophilic archaea: distribution, function, structure, and application

Ryushi Kawakami · Takenori Satomura · Haruhiko Sakuraba · Toshihisa Ohshima

Received: 8 August 2011 / Revised: 11 October 2011 / Accepted: 27 October 2011 / Published online: 17 November 2011

Abstract Dye-linked L-proline dehydrogenase (ProDH) catalyzes the oxidation of L-proline to Δ^1-pyrroline-5-carboxylate (P5C) in the presence of artificial electron acceptors. The enzyme is known to be widely distributed in bacteria and eukarya, together with nicotinamide adenine dinucleotide (phosphate)-dependent (NAD(P)) P5C dehydrogenase, and to function in the metabolism of L-proline to L-glutamate. In addition, over the course of the last decade, three other types of ProDH with molecular compositions completely different from previously known ones have been identified in hyperthermophilic archaea. The first is a heterotetrameric $\alpha\beta\gamma\delta$-type ProDH, which exhibits both ProDH and reduced nicotinamide adenine dinucleotide (NADH) dehydrogenase activity and includes two electron transfer proteins. The second is a heterooctameric $\alpha_4\beta_4$-type ProDH, which uses flavin adenine dinucleotide, flavin mononucleotide, adenosine triphosphate, and Fe as cofactors and creates a new electron transfer pathway. The third is a recently identified homodimeric ProDH, which exhibits the greatest thermostability among these archaeal ProDHs. This minireview focuses on the functional and structural properties of these three types of archaeal ProDH and their distribution in archaea. In addition, we will describe the specific application of hyperthermostable ProDH for use in a biosensor and for DNA sensing.

Keywords Dye-linked L-proline dehydrogenase · Hyperthermophilic archaea · Enzyme complex structure · Flavoenzyme · Catalytic electrode · DNA sensing

R. Kawakami
Analytical Research Center for Experimental Sciences,
Saga University,
1, Honjo-machi,
Saga 840-8502, Japan

T. Satomura
Department of Applied Chemistry and Biotechnology,
Graduate School of Engineering, University of Fukui,
3-9-1 Bunkyo,
Fukui 910-8507, Japan

H. Sakuraba
Department of Applied Biological Science,
Faculty of Agriculture, Kagawa University,
2392 Ikenobe Miki-cho Kita-gun,
Kagawa 761-0795, Japan

T. Ohshima (✉)
Microbial Genetics Division, Institute of Genetic Resources,
Faculty of Agriculture, Kyushu University,
6-10-1 Hakozaki, Higashi-ku,
Fukuoka 812-8581, Japan
e-mail: ohshima@agr.kyushu-u.ac.jp

Introduction

Oxidoreductases catalyze the reversible electron transfer from substrates such as amino acids, alcohols, sugars, and amines and are divided into three main groups: oxidases and oxygenases, which use oxygen as the electron acceptor, and dehydrogenases (reductases), which use nicotinamide adenine dinucleotide (NAD), nicotinamide adenine dinucleotide phosphate (NADP), flavin adenine dinucleotide (FAD), flavin mononucleotide (FMN), pyrroloquinoline quinone, ferredoxin, and cytochrome c as electron acceptors. More than 660 kinds of oxidoreductases playing a variety of important roles in the generation of energy and in the biosynthesis and metabolism of biomolecules have been identified so far (see BRENDA database at http://www.brenda-enzymes.info/). Among them, the NAD- and/or NADP-dependent dehydrogenases, such as alcohol dehydrogenase (EC 1.1.1.1), glucose dehydrogenase (EC 1.1.1.47), and glutamate dehydrogenase (EC 1.4.1.2-4), are abundant and centrally involved in the

metabolism of biomaterials containing sugars, amino acids, and fatty acids. In addition, they have been extensively applied to the production and sensing of biomaterials.

Another group of dehydrogenases, the FAD- and/or FMN-dependent dehydrogenases (EC 1.-.99.-), which include reduced nicotinamide adenine dinucleotide (NADH) dehydrogenase (EC 1.6.99.3) (Dancey et al. 1976; Bergsma et al. 1982; Nisimoto et al. 1986) and succinate dehydrogenase (EC 1.3.99.1) (Davis and Hatefi 1971; Hanstein et al. 1971; Hederstedt et al. 1979), are known to function in energy generation as the primary enzyme in electron transport chains. These enzymes are also called dye-linked dehydrogenases (dye-DHs) because they can utilize artificial dyes such as dichloroindophenol and ferricyanide as electron acceptors instead of their natural acceptors. Dye-DHs have a high potential for utilization as specific elements for electrochemical processing (e.g., in enzyme sensors and batteries) because electrons from the substrate can be introduced to an electrode using an artificial dye as the mediator (Frew and Hill 1987). However, most of these enzymes are associated with cell and/or organelle membranes and must be solubilized from the membranes before their purification and characterization. Once solubilized, they generally exhibit complex molecular architectures, and they are unstable in solution. That has made purification, preservation, and use of dye-DHs very difficult.

On the other hand, enzymes from thermophiles had been shown to be much more stable than their counterparts from mesophiles under a variety of conditions (Adams 1993; Kujo and Ohshima 1998; Li et al. 2005; Ohshima and Soda 1989). It was therefore expected that dye-DHs from thermophiles, in particular hyperthermophiles, which can grow at or near the boiling point of water, may be stable enough to tolerate solubilization and purification. In addition, almost all hyperthermophiles belong to archaea, the third domain of life, and their metabolic pathways and enzymes largely differ from those of mesophilic bacteria and eukarya. Since the middle of 1990s, much effort toward screening strains of hyperthermophilic archaea for dye-DH has been made. To date, several new dye-DHs, including L-proline, D-proline, and D-lactate dehydrogenases, have been identified in the crude extracts of hyperthermophilic archaea, and these hyperthermostable enzymes were successfully purified and characterized (Sakuraba et al. 2001; Satomura et al. 2002, 2008). Among them, the existence of at least three types of L-proline dehydrogenases has been demonstrated. In addition, these enzymes are not membrane-bound, while D-proline dehydrogenase and D-lactate dehydrogenase are membrane-bound, suggesting that L-proline dehydrogenases have great advantage in specific applications to the electrochemical sensing of substrates. In this minireview, we focus on enzymes having dye-DH activity toward L-proline and summarize their molecular characteristics, structures, distributions, and application.

Novel dye-linked L-proline dehydrogenase in hyperthermophilic archaea

Several hyperthermophiles were screened for stable dye-DHs by assessing their activity toward amino acids and organic acids. Using this approach, dye-DH activity toward L-proline was detected in the crude extracts of several *Thermococcus* and *Pyrococcus* strains (Table 1). Dye-linked L-proline dehydrogenases (ProDHs, EC 1.5.99.8) catalyze the oxidation of L-proline to Δ^1-pyrroline-5-carboxylate (P5C) in the presence of artificial electron acceptors such as dichloroindophenol and ferricyanide. They are known to be widely distributed in bacteria and eukarya, where they catalyze the first step in L-proline oxidation to L-glutamate (Fig. 1). A notable example is PutA (proline utilization A), a ProDH from *Escherichia coli* (Scarpulla and Soffer 1978) and *Salmonella typhimurium* (Menzel and Roth 1981a, b). PutA is a membrane-bound dimeric enzyme with a molecular mass of 144 kDa. It catalyzes not only L-proline oxidation to P5C by ProDH but also P5C dehydrogenation to L-glutamate by P5C dehydrogenase (P5CDH), as the two catalytic domains are fused into a single polypeptide chain in this enzyme (Tanner 2008). By contrast, ProDHs from eukarya and from some bacteria are monofunctional enzymes, which are separate from the P5CDH. Analysis of the crystal structures of the ProDH domain of *E. coli* PutA and the full-length protein from *Bradyrhizobium japonicum* PutA revealed the structure of the ProDH domain to have a distorted $(\beta\alpha)_8$ barrel fold (Lee et al. 2003; Srivastava et al. 2010). White et al. (2007) found a monofunctional ProDH in the thermophilic bacterium *Thermus thermophilus* and showed that its crystal structure also consisted of a distorted $(\beta\alpha)_8$ barrel catalytic core domain, as well as a hydrophobic α-helical domain, and that the structure of the catalytic core was similar to PutA, except for the FAD conformation. The 3D structure of eukaryotic ProDH has not yet been determined because it remains difficult to prepare a highly purified enzyme, but it is predicted that the eukaryotic ProDH will also exhibit a barrel fold in its catalytic core, like other

Table 1 ProDH activities in the crude extracts of hyperthermophilic archaea

Strain	Specific activity (U/mg)
Thermococcus profundus	0.023
T. peptonophilus	0.008
T. litoralis	0
Pyrococcus horikoshii	0.014
P. furiosus	0.002
Aeropyrum pernix	0
Sulfobus tokodaii	0
Pyrobaculum islandicum	0

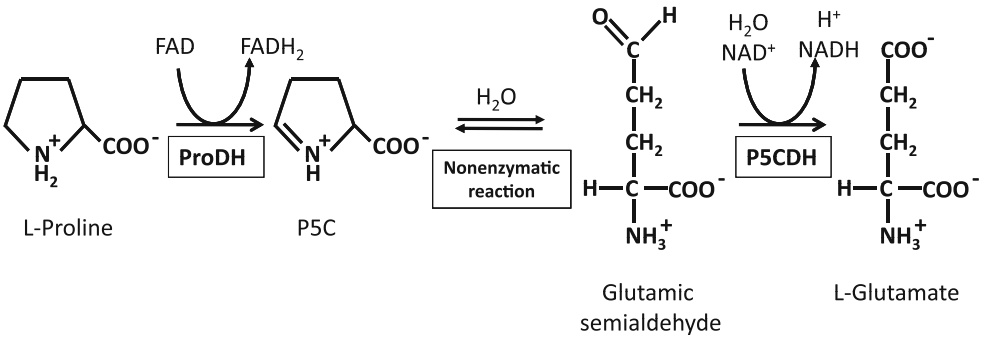

Fig. 1 Oxidation of L-proline to L-glutamate. In the first reaction, L-proline is oxidized to P5C by ProDH. Glutamic semialdehyde, an uncyclized tautomer in spontaneous equilibrium with P5C, is then further oxidized to L-glutamate by P5CDH

monofunctional ProDHs (Zhang et al. 2004; White et al. 2007).

ProDH from the hyperthermophile *Thermococcus profundus*

Because ProDH activity in the crude extract of *T. profundus* was the highest among the hyperthermophiles tested, this microorganism was chosen for purification of ProDH (*Tp*-ProDH) (Sakuraba et al. 2001). Ultracentrifugation analysis indicated that *Tp*-ProDH is not a membrane-bound enzyme, and the enzyme was purified to homogeneity through several column chromatography steps. SDS-PAGE analysis of the purified enzyme revealed that *Tp*-ProDH formed a complex consisting of four different subunits with molecular masses of 54, 42, 19, and 11 kDa, respectively (Kawakami et al. 2004). Moreover, since gel filtration chromatography showed its molecular mass to be about 120 kDa, *Tp*-ProDH was deemed to have a heterotetrameric αβγδ structure. As expected, the enzyme was highly stable, even at high temperatures and at pHs far from neutral pH: the enzyme lost no activity when incubated at 70 °C for 10 min or at 50 °C for 10 min at pH ranging between 4.0 and 10.0. In addition, the enzyme was specific for L-proline; D-proline, L-hydroxyproline, and other amino acids were inert as substrates (Table 2). These results indicate that the ProDH from *T.*

Table 2 Summary of the enzymatic properties of *Tp*-ProDH, *Ph*-ProDH1, and *Pc*-ProDH

	Tp-ProDH[a]	*Ph*-ProDH1[b]	*Pc*-ProDH[c]
Molecular mass			
Native (kDa)	120	440	108
Subunit (kDa)[d]	α: 51.9, β: 42.7 γ: 19.0, δ: 10.6	α: 55.3, β: 42.7	46.3
Structure	αβγδ (heterotetramer)	$\alpha_4\beta_4$ (heterooctamer)	Homodimer
Prosthetic groups	α: FAD, [2Fe–2S] β: FAD	α: ATP, [Fe–4Cys] β: FAD	FAD
	γ: [8Fe–8S]	α/β: FMN	
	δ: [Fe–4Cys][e]		
Substrate	L-Proline, NADH[f]	L-Proline[g]	L-Proline, L-hydroxyproline[h]
Thermostability	70 °C for 10 min	90 °C for 120 min	100 °C for 120 min
K_m values for L-proline (mM)	2.5	4.0	1.7

[a] Sakuraba et al. (2001) and Kawakami et al. (2004)

[b] Kawakami et al. (2005)

[c] Satomura et al. (2011)

[d] Calculated values based on the amino acid sequence

[e] Prediction from the C-terminal sequence of *Ph*-ProDH

[f] Substrates tested for the ProDH activity are as follows: L-proline, D-proline, L-hydroxyproline, sarcosine, D-nopaline, L-ornithine, L-glutamate, L-aspartate, L-arginine, L-lysine, L-serine, L-leucine, L-valine, L-alanine, and glycine, and those for the NADHDH activity are as follows: NADH, NADPH, sarcosine, and D-nopaline

[g] Substrates tested: substrates listed in footnote f, hydroxyl-D-proline, pyrrolidone-5-carboxylate, pyrrole-2-carboxylate, and pipecolic acid

[h] Substrates tested: substrates listed in footnote f, except for D-nopaline, L-aspartate, L-lysine, and glycine

profundus is a novel ProDH complex that is highly stable, as compared to other known dye-DHs.

For more detailed characterization of *Tp*-ProDH, its gene was cloned and expressed in an *E. coli* expression system, which revealed that the genes *pdhA*, *pdhB*, *pdhF*, and *pdhX*, encoding the α, β, γ, and δ subunits, respectively, were tandemly arranged as a gene cluster in the order *AFXB* with the 3′-end of the upstream gene overlapping the 5′-end of the next gene (Kawakami et al. 2004). Functional analysis of each subunit revealed that only the β subunit had ProDH activity, indicating that the ProDH reaction was substantially catalyzed by the β subunit within the enzyme complex. Interestingly, the α subunit exhibited activity like that of a dye-linked NADH dehydrogenase (NADHDH), which catalyzes the oxidation of NADH to NAD. The same activity was also detected within the enzyme complex and was not detected in the other subunits. As mentioned above, PutA catalyzes the oxidation of L-proline to L-glutamate through sequential reactions catalyzed by its ProDH and P5CDH domains. However, there has been no other report of an enzyme (or enzyme complex) catalyzing the dehydrogenation of two independent substrates. An adenine-binding motif is conserved in the N-terminal regions of both the α and β subunits, and FAD could bind in this region (also see Fig. 4). In addition, another adenine-binding motif is conserved in the middle of the α subunit sequence, suggesting binding of substrate NADH. A [2Fe–2S] iron–sulfur cluster (ISC) motif containing four cysteine residues is conserved in the N-terminal of the α subunit. An ISC motif is also conserved in the γ subunit, which has two [4Fe–4S] cluster motifs, and based on the results of a homology search, the γ subunit is predicted to be a ferredoxin-like electron transfer protein. The δ subunit, which is the smallest, showed homology with only hypothetical proteins encoded by similar gene clusters observed in other *Thermococcus* and *Pyrococcus* genomes and had a four-cysteine region in its sequence. The δ subunit is also predicted to be an electron transfer protein (see below for details). In sum, the αβγδ-type ProDH complex from *T. profundus* is a novel FAD-containing, bifunctional dehydrogenase complex that consists of a ProDH, a NADHDH, and two electron transfer proteins (Fig. 2).

Presence of two different ProDHs in *Pyrococcus horikoshii*

While using ProDH activity staining to screen for dye-DHs, two different mobility bands were observed on the native-PAGE of crude extracts from *Thermococcus peptonophilus* and *P. horikoshii* (Fig. 3). It appeared that these hyperthermophilic archaea produced two different types of ProDH: ProDH1 (less mobility) and ProDH2 (larger mobility). This was confirmed when both enzymes (*Ph*-ProDH1 and *Ph*-ProDH2) were successfully purified to homogeneity from *P. horikoshii* cell extract and characterized separately (Kawakami et al. 2005). SDS-PAGE revealed *Ph*-ProDH2 to be composed of four different subunits (α, β, γ, and δ). Moreover, comparison of the N-terminal sequences of the subunits with gene sequences obtained from the genome data (Kawarabayasi et al. 1998) enabled the genes encoding the α, β, γ, and δ subunits to be identified as *PH1749*, *PH1751*, *PH1750*, and *PH1750.1n*, respectively, which form a gene cluster. Each amino acid sequence deduced from the four genes showed high homology with those of the corresponding subunit in *Tp*-ProDH, indicating that *Ph*-ProDH2 is the same type of ProDH as *Tp*-ProDH. By contrast, SDS-PAGE of *Ph*-ProDH1 showed only two different subunits with molecular masses of 56 and 43 kDa, and the encoding genes were identified as *PH1363* and *PH1364*, respectively, from the N-terminal amino acid sequences. Using gel filtration, the molecular mass of *Ph*-ProDH1 was determined to be about 440 kDa, which indicates that *Ph*-ProDH1 is a second novel ProDH complex with a heterooctameric $\alpha_4\beta_4$ structure (Kawakami et al. 2005). Like *Tp*-ProDH, *Ph*-ProDH1 catalyzes the exclusive oxidation of L-proline to P5C, but exhibits greater thermostability with no loss of

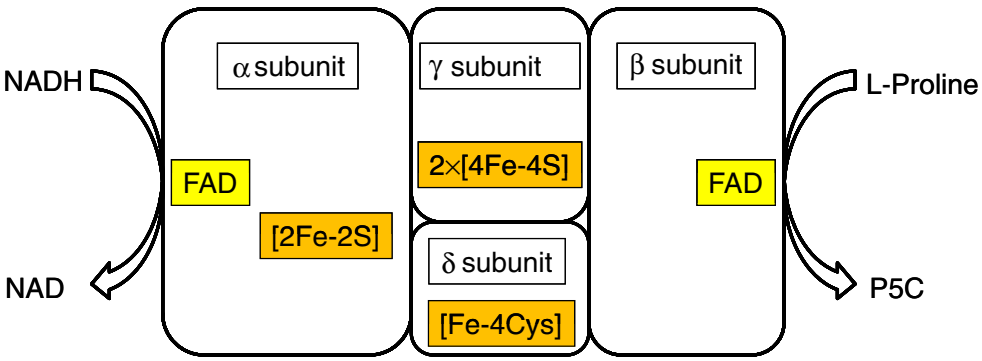

Fig. 2 Postulated scheme for the *Tp*-ProDH complex

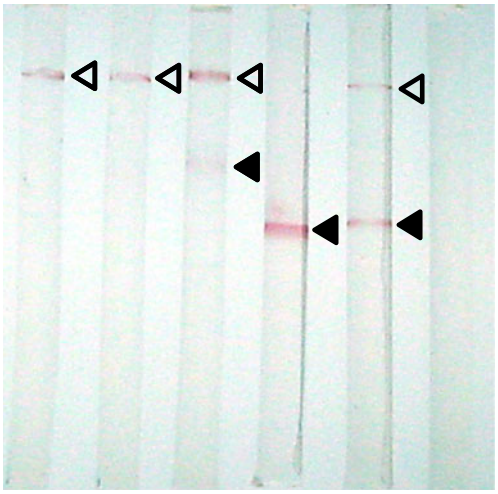

Fig. 3 Active staining for ProDH in crude extracts from *Thermococcales* strains. From *left* to *right*: *P. abyssi*, *P. furiosus*, *P. horikoshii*, *T. profundus*, *T. peptonophilus*, and *Thermococcus litoralis*. *Open* and *filled triangles* show $\alpha_4\beta_4$-type and $\alpha\beta\gamma\delta$-type ProDHs, respectively. Neither active band was detected in *T. litoralis*. Active staining was performed described by Kawakami et al. (2005)

activity when incubated at 90 °C for 120 min (Table 2). The *Ph*-ProDH activity was detected only in the β subunit, but no NADHDH activity was detected in either the enzyme complex or the α subunit.

The primary structure of the β subunit of *Ph*-ProDH1 showed a high degree of similarity (65%) to that of *Tp*-ProDH, which had an adenine-binding motif in its N-terminal region (Fig. 4a). On the other hand, the α subunit of *Ph*-ProDH1 had one adenine-binding motif and a four-cysteine cluster region that was similar to the sequence of the δ subunit of *Tp*-ProDH, in its N- and C-terminal, respectively (Fig. 4b). HPLC analysis of *Ph*-ProDH1 extract showed the presence of FAD, FMN, and adenosine triphosphate (ATP) as cofactors, which is totally different from *Tp*-ProDH, which contains only FAD. Adenosine diphosphate (ADP) is reportedly present on trimethylamine dehydrogenase (Lim et al. 1988), but there have been no other reports of the presence of ATP on a dehydrogenase. After the α and β subunits were independently purified from two different cultures of recombinant *E. coli* cells, the presence of ATP, FAD, and FMN on the two subunits was examined by HPLC. The results showed that ATP and FAD bind to the α and β subunits, respectively, but FMN was not detected in either subunit. As is described in the following section, the crystal structure of *Ph*-ProDH1 clearly shows why FMN is not detected on the separate subunits.

In that regard, Monaghan et al. (2007) reported on the mechanism and redox properties of the $\alpha_4\beta_4$-type ProDH from *Pyrococcus furiosus*. Like *Ph*-ProDH1, this enzyme also contains FAD, FMN, and ATP as cofactors, but unlike *Ph*-ProDH1, ATP and FMN were easily released from the enzyme by exchanging the potassium phosphate buffer. Moreover, by measuring FAD reduction upon addition of substrate under anaerobic conditions, it was determined that the $\alpha_4\beta_4$-type ProDH from *P. furiosus* catalyzes the oxidation of L-pipecolic acid and sarcosine, as well as L-proline.

Crystal structure of $\alpha_4\beta_4$-type L-proline dehydrogenase

To obtain structural information about $\alpha\beta\gamma\delta$-type *Tp*-ProDH and $\alpha_4\beta_4$-type *Ph*-ProDH1, crystallization of the two enzyme complexes was endeavored. As a result, a high quality crystal of *Ph*-ProDH1was successfully generated, and subsequent X-ray analysis enabled to determine the protein's 3D structure with 2.8 Å resolution (Tsuge et al. 2005). *Ph*-ProDH1 assembled as a tetramer of the asymmetric unit, which was an $\alpha\beta$ heterodimer. Two $\alpha\beta$ heterodimers were linked by an intermolecular disulfide bond between the C381 residues in the α subunits, and the resulting $(\alpha\beta)_2$ heterotetramer bound to a second tetramer to form the heterooctamer (Fig. 5a, b).

The ProDH catalytic (β) subunit contains an FAD-binding domain and an interface domain for interaction with the α subunit. The FAD-binding domain contains a dinucleotide-binding fold also observed in enzymes belonging to the glutathione reductase family (Dym and Eisenberg 2001). This means that the structure of the ProDH domain of *Ph*-ProDH1 is completely different from those of PutA and bacterial monofunctional ProDHs, which have a $(\beta\alpha)_8$ barrel fold (Lee et al. 2003; Srivastava et al. 2010; White et al. 2007). The crystal structure also showed that FMN is located at the interface between the α and β subunits and that the isoalloxyazine ring of FMN is laid almost parallel to that of FAD at a distance of 12.5 Å (Fig. 5c). The clear implication of this observation is that FMN would not be detected on the α and β subunits produced independently in *E. coli* because FMN binds to the enzyme through hydrophobic interactions when sandwiched between the two subunits. ATP was found to be situated within the α subunit in the dinucleotide-binding domain. The α subunit also contains a four-cysteine cluster domain (C413, C415, C447, and C452), within which C413 and C452 form a disulfide bond, and C447 is in close proximity to the disulfide (Fig. 5c). Although the presence of an ISC in this domain could not be confirmed from this analysis, iron was detected within the enzyme complex using a colorimetric method as well as an inductively coupled plasmaspectrometer, and an electron density was confirmed near the C413–C452 disulfide bond at 5σ. These results suggest that iron is present in the cysteine cluster

a

```
TpProDH-beta      1 -MRSEAKTVIIGGGIIGLSIAYNLAKLGESDVVVLEKGYLGN--GSTFRCGTGIRQQFND
PhProDH1-beta     1 MLPEKSEIVVIGGGIVGVTIAHELAKRGE-EVTVIEKRFIGS--GSTFRCGTGIRQQFND
PcProDH           1 ----MYDYVVVGAGVVGMATAFHIKRLAPRAKVLVVDQNVGVGMGDTARSAAAFRTIFTS
                      * ***** *  **  *** **  * * **   *   ***************

TpProDH-beta     58 EANIRMMKRSVELWKGLSEELGMDVEFTQSGYLFLIYEK---------DELEAFKNNVRL
PhProDH1-beta    58 EANVRVMKRSVELWKKYSEEYGFS--FKQTGYLFLLYDD---------EEVKTFKRNIEI
PcProDH          57 WINRALAKSSVDFYR-SVQSRGVDLGMRFVGYLFLVPEESREAMLKVVEELRRMGVGVDV
                    *** * *********  *** *    * * ***** *           *   ** *

TpProDH-beta    109 QNRFGVPSRIITPEEAKEIVPPLNTNGVIAAAWNHTDGKANPFKAVFAYAEAAKRLGVEI
PhProDH1-beta   107 QNKFGVPTKLITPEEAKEIVPLLDISEVIAASWNPTDGKADPFEATTAFAVKAKEYGAKL
PcProDH         115 FEKLDMPIRFRVRDD--EEAREMGLPDVAFSILVRDAGIIDPERVVRYYYEQYLNEGGEV
                    ** ****   ********** *    **** ** ***** ** *  * *  **  *

TpProDH-beta    169 YEYTEAKDIRVE--------------EGKIKTVVTNRGEIKTGRVINAANAWAPLINKM
PhProDH1-beta   167 LEYTEVKGFLIE--------------NNEIKGVKTNKGIIKTGIVVNATNAWANLINAM
PcProDH         174 LFNAKVESVAFSPKRPIGIPGEPFPWQDVKVRGVETTAGFVEAKNVVLATGAWTERLADA
                     **** *    *                  ** * ** * **** * ** **** *** *

TpProDH-beta    214 AGVPIKIPIEPYKHQGVKTEPIKPGQIEPMVIS----------FKHGGVYLTQEAYQGGV
PhProDH1-beta   212 AGIKTKIPIEPYKHQAVITQPIKRGTINPMVIS----------FKYGHAYLTQT-FHGGI
PcProDH         234 LGFG--LPIKPRKRQVFVVN--AEGELEDLLLSGLAERYAPMIILPRGIYIRPEPSEKTF
                    **   ********** * * *** * * *****          ** *  ****    **

TpProDH-beta    264 IGGYGLKYGPTYDITP---TYEFLRGVSYRFSQIIPALKYVNVIRIWGGFYAE-TPDHNA
PhProDH1-beta   261 IGGIGYEIGPTYDLTP---TYEFLREVSYYFTKIIPALKNLLILRTWAGYYAK-TPDSNP
PcProDH         290 WIGVADRRPYRFEDPPEPEETLWRYGIYPVLTKYVPAFEGKTPQAAWAGHYDENVVDYQP
                    *** *   ***** **   ****** *** *  ******     * * * **  *** *

TpProDH-beta    320 AIGRINEIDEFYIAAGFSGHGFMLAPAVAEALAEFIVDGKTDKPLDFYDPYRFERGELRG
PhProDH1-beta   317 AIGRIEELNDYYIAAGFSGHGFMMAPAVGEMVAELITKGKTKLPVEWYDPYRFERGELRT
PcProDH         350 IVDRLAEG--LYIAAGTSGSGIMKADAVGRIAAYLALG---YEKAELYGGTVVESNVLKA
                    ***** *    ************ **** *  ** *  ***  *   ************

TpProDH-beta    380 QALQMG-----
PhProDH1-beta   377 AALQMG-----
PcProDH         405 NRCLEPERLVI
                     *****
```

Fig. 4 **a** Alignment analysis of the ProDH subunits from *Tp*-ProDH, *Ph*-ProDH1, and *Pc*-ProDH. Identical residues among these subunits are shown in *boxes* and those between β subunits from *Ph*-ProDH1 and *Tp*-ProDH are shown with *asterisks*. Adenine-binding motif is depicted with *light background*. **b** Alignment analyses of the α subunit of *Ph*-ProDH1 with those from *Ph*-ProDH2 and *Tp*-ProDH. The C-terminal sequences of these enzymes were also compared with the sequences of δ subunits from *Ph*-ProDH2 and *Tp*-ProDH. Identical residues among the α subunits are shown with *asterisks* and those between α and δ subunits are shown in *boxes*. A [2Fe–2S] ISC region and adenine-binding motifs are depicted with *dark* and *light backgrounds*, respectively

domain of the α subunit, where it forms a [Fe–4Cys] cluster. The [Fe–4Cys] cluster can easily be oxidized during the crystallization process. The position of the cysteines in the sequence in this region corresponds to that of the δ subunit of *Tp*-ProDH (Fig. 4b), suggesting the δ subunit also has a [Fe–4Cys] cluster and functions as an electron transfer protein.

This cluster is located near the FMN at a distance of 11.7Å. The positions of the FAD, FMN, and four-cysteine cluster domain prompted us to speculate that a novel electron transfer system is formed within the structure of the complex (Fig. 5c). The electrons obtained through oxidation of L-proline are received by FAD on the β subunit and then transferred to the cysteine cluster domain in the α subunit via FMN. C47β, W304β, and M444α may also be associated with this electron transfer system. In addition, CAPS used in the crystallization buffer was bound within a hydrophobic domain consisting of four tryptophans and a valine residue in the α subunit and may be a binding region for an unidentified physiological electron acceptor (Fig. 5b). Finally, it is proposed that a physiological electron acceptor binding within this hydrophobic domain receives electrons transferred to the cysteine cluster domain. To test that idea, it

b

```
TpProDH-alpha      1 MRLTEHPILDFSERRGRKVTIHFEGQPVEAYEGETIAMALHAAGIRVLSHSAEKHRPRGL
PhProDH2-alpha     1 MRINEHPILDFEKKRKRKVTIYYKGQPIEAYEGETIAAALHAAGIRVLNYSRVRKRPRGL
PhProDH1-alpha     1 -----MRPLDLTEKRGKKVTIYFEGKELEAYEGEKLPVALLANEIYWLTTSNEG-RKRGA
                       **    *  ****   *   ******    ** *  *  *  *    * **

TpProDH-alpha     61 FCAIGKCSSCLVKVNGVPNVRSCITLVEEGMKVEMQRGKETLPKGA-KPPAWKDAPRYKA
PhProDH2-alpha    61 FCAIGKCSSCLMTVNGIPNVRTCITLVEDGMKIEEN--KPILPANINKKDKKKRAKIVKG
PhProDH1-alpha    55 FTFG----PVPMTVNGVKGLEARRIKVKDGMKIERQ---GYYDFHEEPVVEPGEIERVVV
                     *           ***          *  *** *

TpProDH-alpha    120 DVVVIGGGPAGLMAAIHAADAGASVILIDENPMLGGQLVKQTHKFFGKREQFAGVRGVKI
PhProDH2-alpha   119 DIIVVGGGPAGMMAAISASDTGAKVILIDESPMLGGQLVKQTHKFFGKRDQFAGIRGIKI
PhProDH1-alpha   108 DVAIIGGGPAGIGAALELQQY-LTVALIEERGWLGGDMWLKGIKQEGFNKDSR-----KV
                     *    ******  **         * ** *   ***       *  *          *

TpProDH-alpha    180 AEILGEEVKKRGNIEVFLETSAVGVFHEGEEKLVAAVRKNKELLEFLGKTLVVATGAMEK
PhProDH2-alpha   179 AEILRREIEKRENIKAYLRTSAVGIFQDGEEKLVIGVRKENELIEFKGKAVIVATGAMEK
PhProDH1-alpha   162 VEELVGKLN--ENTKIYLETSALGVFDKGEYFLVPVVRGDK-LIEILAKRVVLATGAIDS
                      * *        *    * *** * *  **  **  **    * *   *    ****

TpProDH-alpha    240 MIPFENNDLPGIYGAGAIQTLMNTYGVKPGDRVLIVGAGNVGLILAYQLIQAG---VEVK
PhProDH2-alpha   239 TIPFENNDLPGIYGAGAIQTLMNTYGIKPGEKALIVGAGNVGLILAYQLLQAN---VQVQ
PhProDH1-alpha   219 TMLFENNDMPGVFRRDFALEVMNVWEVAPGRKVAVTGSKADEVIQELERWGIDYVHIPNV
                        ***** **          **     **      *      *

TpProDH-alpha    297 AIVEAMPKVGGYFVHAAKVRRLGVPILTR------HTILRAEGKDRVERAVIAQLDENWR
PhProDH2-alpha   296 AIVEAMPKIGGYFVHAAKVRRLGVPILTR------HTILKAEGEEKVERAIVAEIDENWN
PhProDH1-alpha   279 KRVEGNEKVERVIDMNNHEYKVDALIFADGRRPDINPITQAGGKLRFRRGYYSPVLDEYH
                      **   *                  *          *  * *     *

TpProDH-alpha    351 PVPGTEKVFEVDTIALAVGLRPSIELLHQAGCQVKFVRELSGHVAVRDGRMETTVQGIFV
PhProDH2-alpha   350 PIPGTEKIFDVDLIAIAVGLRPSIELLQQAGCQIKYVRELGGHVPVRDRWMETTVKGIFV
PhProDH1-alpha   339 RIK--DGIYVAGSAVSIKPHYANYLEGKLVGAYILKEFGYDAQPCIYEEKLREYEPESLS
                                                 *

TpProDH-alpha    411 AG----DSAGIEEATTAML-EGKIAGIAAALKAGAASPEWLAEIEKAQRDLLEFRSGPFG
PhProDH2-alpha   410 AG----DTAGIEEATTAML-EGKIAGLAAALRLGIAGEEWVKEIEKTEKELEEFRSGPFG
PhProDH1-alpha   397 IPRIPLDKFNLEDVQICGC-DVSLKKVDEVIRKGITDLQIIKRLTHLAMGFCQGRYCLFN
TpProDH-delta      1      MTEDPKGKIIICRCNDVTLKEIEDLIEGGITDIEEIKRLTRIGMGPCQGRTCIPL
PhProDH2-delta     1      MK-------IVCRCNDVTLEEIEKLIDEGVTDLEELRRLLRIGMGPCQGRTCIPI
                         *    *                    *                      *   *

TpProDH-alpha    466 RHVLEG------------------IKKVLVGVDGYA
PhProDH2-alpha   465 RRVIEG------------------IKKLLEGSK---
PhProDH1-alpha   456 GAVVVSQRTGKKLSEIDLPVARSPIKNVKMGILARR-------
TpProDH-delta     56 VISIIARKAGKKPGEIPVPATRVPVRPVMMGVLAGEMGDDDEE
PhProDH2-delta    49 VISILARKTGKKPEEISLPNARFPIRPVRIEAFIEE---EDEK
                       *                    **    *
```

Fig. 4 (continued)

will be necessary to identify the residues associated with this pathway and the physiological electron acceptor. It will also be necessary to analyze the unbroken structure of the cysteine cluster domain and to clarify the role of ATP bound to the α subunit, which is currently predicted to be involved in stabilizing the structure or in regulating the electron transfer and not to be an essential factor for the catalysis.

In sum, *Ph*-ProDH1 is a second novel FAD-, FMN-, and ATP-containing ProDH complex, which forms an $\alpha_4\beta_4$ structure. Like αβγδ-type *Tp*-ProDH, the L-proline dehydrogenation is catalyzed by 42 kDa β subunit in this enzyme. Unlike αβγδ-type ProDH, α subunit of *Ph*-ProDH1 does not exhibit the NADHDH activity and creates a new electron transfer pathway formed by FMN-binding domain, [Fe–4Cys] cluster domain, and hydrophobic domain.

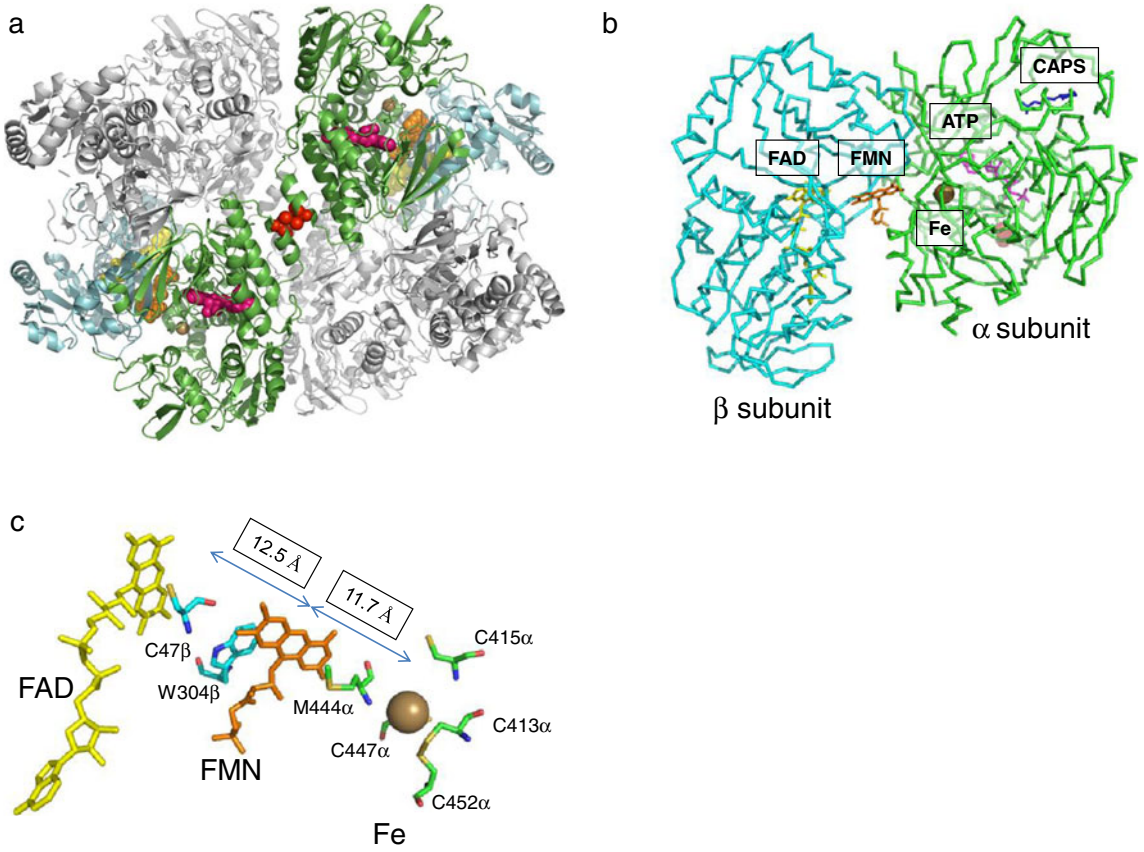

Fig. 5 Crystal structure of *Ph*-ProDH1 (PDB ID: 1Y56). Overall structure of the heterooctameric $(\alpha\beta)_4$ structure (**a**). The forward $(\alpha\beta)_2$ set is shown in *green* and *cyan*, respectively. Another $(\alpha\beta)_2$ set is shown from the back side in *gray*. In the forward set, FAD, FMN, ATP, and Fe are depicted in *yellow*, *orange*, *magenta*, and *ocher*, respectively. The disulfide bridge between C381s is in *red sphere*. Heterodimeric αβ structure (**b**). CAPS is depicted in *blue*; others are the same colors used in **a**. Structural relationships among FAD, FMN, and Fe (**c**)

A third type of L-proline dehydrogenase from *Pyrobaculum calidifontis*

A third type of ProDH isozyme has been identified in the aerobic hyperthermophilic archaeon *P. calidifontis* (*Pc*-ProDH), and interestingly, some of the enzymatic properties of this enzyme differ completely from those of αβγδ-type *Tp*-ProDH and $\alpha_4\beta_4$-type *Ph*-ProDH1 (Satomura et al. 2010). The molecular mass of the native enzyme and its subunit was estimated to be 108 and 46.3 kDa using gel filtration and SDS-PAGE, respectively, which indicates that the enzyme forms a homodimer (Table 2). The gene encoding *Pc*-ProDH was determined to be *Pcal_1655*, based on its N-terminal amino acid sequence, and it did not form a gene cluster like the αβγδ- and $\alpha_4\beta_4$-type ProDHs. The amino acid sequence of the enzyme contained an adenine-binding motif in its N-terminal region, but it exhibited only a small degree of identity (<26%) with those of the active components (β subunit) of the *Tp*-ProDH and *Ph*-ProDH1 complexes (Fig. 4a).

Pc-ProDH catalyzes the dehydrogenation of both L-proline and L-hydroxyproline (relative activity, 72% as compared to L-proline). By contrast, neither *Tp*-ProDH nor *Ph*-ProDH1 is able to catalyze the dehydrogenation of L-hydroxyproline. Thus, *Pc*-ProDH exhibits relatively broad substrate specificity, as compared to the ProDHs from hyperthermophiles described so far. In addition, the *Pc*-ProDH enzyme remains active after incubation at 100 °C for 120 min, making it the most thermostable ProDH identified so far.

Application for ProDH to an L-proline sensor and a DNA sensing system

As mentioned above, dye-DHs have the potential for use as a specific element in biosensors functioning on the basis of electrochemical detection (Frew and Hill 1987). However, the use of dye-DHs in such applications was precluded by their lack of stability. However, the ProDHs from hyperthermophilic archaea are highly thermostable and can be efficiently produced and purified from a well-established recombinant *E. coli* expression system. As a first step, an electrochemical L-proline detection system using *Tp*-ProDH

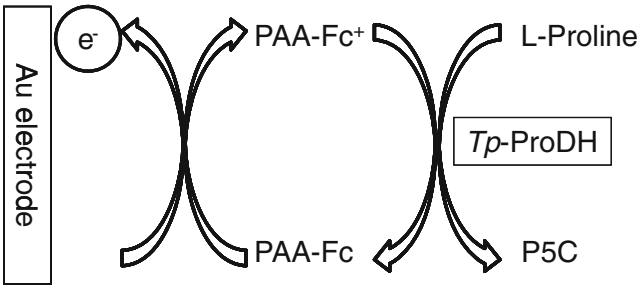

Fig. 6 Scheme for the electrochemical detection of L-proline using *Tp*-ProDH with a polymerized mediator (poly(allylamine) ferrocene, *PAA-Fc*)

was constructed. In this system, *Tp*-ProDH is immobilized on a gold electrode along with a polymerized mediator using an electrostatic layer-by-layer adsorption method, which enabled amperometric detection of L-proline (Fig. 6) (Zheng et al. 2006). In addition, multiwalled carbon nanotubes were tested as mediators in an effort to improve the sensitivity of the electrochemical L-proline detection (Zheng et al. 2010). A glassy carbon electrode modified with carbon nanotubes and *Tp*-ProDH exhibited an apparent catalytic response to L-proline, and both the amperometric response and the applied potential were greatly improved, as compared to the gold electrode modified with a polymerized mediator. In addition, the apparent K_m value (0.33 mM) for L-proline of the immobilized ProDH mediated with the carbon nanotubes was lower than that of free *Tp*-ProDH (2.05 mM) in the presence of dichloroindophenol serving as an electron acceptor. These reports describe the first application in which a thermostable dye-DH was utilized as a functional element in a biosensor. In general, the use of hyperthermophilic enzyme has the advantage of thermostability and the disadvantage of low activity at low temperature. However, the aforementioned improved detection system was enough to detect the amperometric response even at room temperature (20 °C). This indicates that, at least in the application to the sensor element, the hyperthermophilic dye-DH has potential usefulness at ordinary temperature. The conventional sensors employing mesophilic enzymes still have serious problems, such as a lack of long-term stability caused from deactivation of the immobilized enzymes and an inactivation of the enzymes during the immobilization processes. Utilization of dye-DHs from hyperthermophiles as a biosensor element has been expected to overcome these problems and have greater capability for practical applications than the counterparts from mesophiles.

Recently, a DNA sensing system that makes use of *Tp*-ProDH has been developed. This system is based on a combination of DNA hybridization and electrochemical detection and is divided into three steps: (1) amplification of the target DNA by PCR; (2) hybridization of the target DNA to an enzyme-labeled probe and to an electrode-bound capture probe, both of which are designed to contain nucleotide sequences complementary to sequences on opposite sides of the target DNA; and (3) amperometric determination through the enzyme reaction. Because the hybridization step requires treatment at a high temperature (about 94 °C), the enzyme used must be highly thermostable. The new system was constructed for detection of *Legionella* species (Fig. 7), which cause a type of human pneumonia, Legionnaires disease. In this system, mip DNA encoding a specific toxic protein from *Legionella* was used as the target DNA (Engleberg et al. 1989). The amplified mip gene, a *Tp*-ProDH-labeled probe, and a biotin-labeled capture probe were mixed on a carbon electrode modified with avidin, heated for 1 min at 94 °C, and then immediately cooled to room temperature. In this process, the biotin-labeled capture probe is bound to the carbon electrode through a biotin–avidin interaction and to the mip gene through DNA hybridization. The *Tp*-ProDH-labeled probe is also hybridized to the opposite side of the mip gene. After the unbounded probe is washed away, electrochemical responses proportional to the amount of bound ProDH are obtained in the presence of L-proline. Breakouts of pneumonia-causing *Legionella* species generally occur in spas and hospitals (Diederen 2008). At present, *Legionella* species are detected through selective cultivation, and it takes about 2 weeks to identify the microorganisms. By contrast, the organism could be identified using a new system within a few hours.

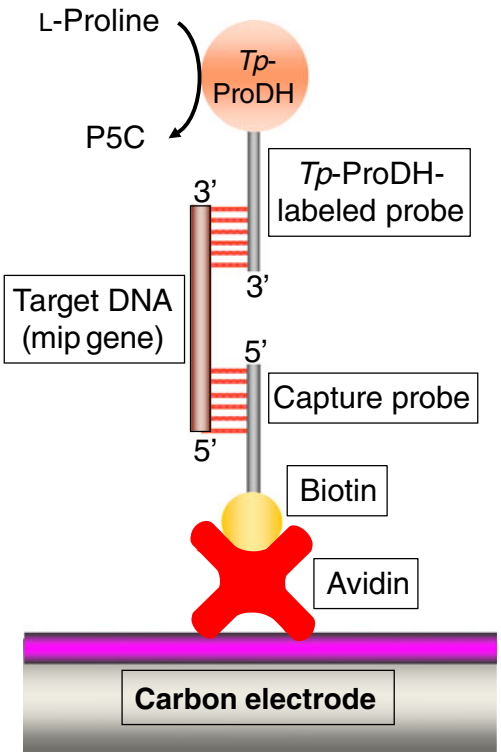

Fig. 7 Scheme for a DNA sensing system using *Tp*-ProDH

Distribution of ProDHs in archaea

As described above, two different types of ProDH complex have been found so far in the hyperthermophilic archaea *T. profundus* and *P. horikoshii*. The genomes of 111 archaeal species are currently open in the Kyoto Encyclopedia of Genes and Genomes (KEGG) database (http://www.genome.jp/kegg/). Information on only three genomes from *Pyrococcus* species within *Thermococcales* was available in 2004 (Kawarabayasi et al. 1998; Maeder et al. 1999; Cohen et al. 2003), when the existence of two different ProDHs in *P. horikoshii* was discovered. Since then, the genomes of eight additional *Thermococcus* and *Pyrococcus* species have opened (Fukui et al. 2005; Lee et al. 2008, 2011; Mardanov et al. 2009; Zivanovic et al. 2009; Vannier et al. 2011; Jun et al. 2011). Moreover, as a result of gene cluster searches for *Ph*-ProDH1 ($\alpha_4\beta_4$-type) and *Ph*-ProDH2 ($\alpha\beta\gamma\delta$-type) in the KEGG database, all of the *Thermococcales* species are now known to have similar gene clusters in their genomes. Although only the activity of a $\alpha\beta\gamma\delta$-type ProDH was observed in the crude extract of *T. profundus*, a gene cluster for the $\alpha_4\beta_4$-type of ProDH was found upstream of the $\alpha\beta\gamma\delta$-type gene cluster, which is similar to the case of *Thermococcus kodakaraensis* (unpublished data). In addition, a gene cluster encoding $\alpha_4\beta_4$-type ProDH was also observed in the genomes of both *Sulfolobus* and *Metallospaera* species, and genes encoding $\alpha\beta\gamma\delta$-type ProDH have been detected in other archaea, including *Archaeoglobus*, *Staphylothermus*, and *Acidprofundum*, as well as in bacteria such as *Thermanaerovibrio* and *Kosmotoga*, though fragmentation or combination of the genes and pseudogene formation were observed in some of these bacterial clusters. Taken together, these results are indicative of the wide distribution of $\alpha_4\beta_4$-type and $\alpha\beta\gamma\delta$-type ProDHs among archaea. As shown in Fig. 3, several hyperthermophilic archaea do not show the ProDH activities in their cell extracts, although the genes encoding the enzymes are present in their genomes. In some cases, the ProDH genes may not be constitutively expressed in the cells under used cultivation conditions. Thus, it will be necessary to determine suitable conditions for their gene expression. This will lead to better understanding for the physiological roles of the hyperthermophilic ProDHs.

Recently, a homodimeric ProDH (i.e., a third type of ProDH) has been also identified in the aerobic hyperthermophilic archaeon *P. calidifontis*. A *Pc*-ProDH homologue was also found in *Pyrobaculum*, *Thermoproteus*, and *Thermoplasma* species, and in *Aeropyrum pernix*. It was recently revealed that the *APE1267.1* gene product in *A. pernix*, which has 43% sequence identity with *Pc*-ProDH, also shows ProDH activity and formed crystals enabling structural analysis at 2.9 Å resolution (Satomura et al. 2011).

Although there are no proteins homologous to PutA in archaea, proteins homologous to bacterial monofunctional ProDH can be found in the KEGG database. These include ProDH homologues from halophilic archaea such as *Haloarcula*, *Haloferax*, and *Halobacterium*.

To date, three different ProDH isozymes in hyperthermophilic archaea have been identified, but their physiological functions in L-proline metabolism remain unclear. More detailed structural analyses, identification of the physiological electron acceptors, and assessment of the effects of gene disruption will increase our understanding of the physiological function of these ProDH isozymes.

Acknowledgments We thank Prof. Hideaki Tsuge for his excellent work to the structural analysis of *Ph*-ProDH1. We also thank Prof. Shin-ichiro Suye and his students for their crucial contributions to the application of ProDH.

References

Adams MW (1993) Enzymes and proteins from organisms that grow near and above 100 degrees C. Annu Rev Microbiol 627–658

Bergsma J, Van Dongen MB, Konings WN (1982) Purification and characterization of NADH dehydrogenase from *Bacillus subtilis*. Eur J Biochem 128:151–157

Cohen GN, Barbe V, Flament D, Galperin M, Heilig R, Lecompte O, Poch O, Prieur D, Quérellou J, Ripp R, Thierry JC, Van der Oost J, Weissenbach J, Zivanovic Y, Forterre P (2003) An integrated analysis of the genome of the hyperthermophilic archaeon *Pyrococcus abyssi*. Mol Microbiol 47:1495–1512

Dancey GF, Levine AE, Shapiro BM (1976) The NADH dehydrogenase of the respiratory chain of *Escherichia coli*. I. Properties of the membrane-bound enzyme, its solubilization, and purification to near homogeneity. J Biol Chem 251:5911–5920

Davis KA, Hatefi Y (1971) Succinate dehydrogenase. I. Purification, molecular properties, and substructure. Biochemistry 10:2509–2516

Diederen BM (2008) *Legionella* spp. and Legionnaires' disease. J Infect 56:1–12

Dym O, Eisenberg D (2001) Sequence-structure analysis of FAD-containing proteins. Protein Sci 10:1712–1728

Engleberg NC, Carter C, Weber DR, Cianciotto NP, Eisenstein BI (1989) DNA sequence of mip, a *Legionella pneumophila* gene associated with macrophage infectivity. Infect Immun 57:1263–1270

Frew JE, Hill HA (1987) Electrochemical biosensors. Anal Chem 59:933A–944A

Fukui T, Atomi H, Kanai T, Matsumi R, Fujiwara S, Imanaka T (2005) Complete genome sequence of the hyperthermophilic archaeon *Thermococcus kodakaraensis* KOD1 and comparison with *Pyrococcus* genomes. Genome Res 15:352–363

Hanstein WG, Davis KA, Ghalambor MA, Hatefi Y (1971) Succinate dehydrogenase. II. Enzymatic properties. Biochemistry 10:2517–2524

Hederstedt L, Holmgren E, Rutberg L (1979) Characterization of a succinate dehydrogenase complex solubilized from the cytoplasmic membrane of *Bacillus subtilis* with the nonionic detergent Triton X-100. J Bacteriol 138:370–376

Jun X, Lupeng L, Minjuan X, Oger P, Fengping W, Jebbar M, Xiang X (2011) Complete genome sequence of the obligate piezophilic hyperthermophilic archaeon *Pyrococcus yayanosii* CH1. J Bacteriol 193:4297–4298

Kawakami R, Sakuraba H, Ohshima T (2004) Gene and primary structures of dye-linked L-proline dehydrogenase from the hyperthermophilic archaeon *Thermococcus profundus* show the

presence of a novel heterotetrameric amino acid dehydrogenase complex. Extremophiles 8:99–108

Kawakami R, Sakuraba H, Tsuge H, Goda S, Katunuma N, Ohshima T (2005) A second novel dye-linked L-proline dehydrogenase complex is present in the hyperthermophilic archaeon *Pyrococcus horikoshii* OT-3. FEBS J 272:4044–4054

Kawarabayasi Y, Sawada M, Horikawa H, Haikawa Y, Hino Y, Yamamoto S, Sekine M, Baba S, Kosugi H, Hosoyama A, Nagai Y, Sakai M, Ogura K, Otsuka R, Nakazawa H, Takamiya M, Ohfuku Y, Funahashi T, Tanaka T, Kudoh Y, Yamazaki J, Kushida N, Oguchi A, Aoki K, Kikuchi H (1998) Complete sequence and gene organization of the genome of a hyper-thermophilic archaebacterium, *Pyrococcus horikoshii* OT3. DNA Res 5:55–76

Kujo C, Ohshima T (1998) Enzymological characteristics of the hyperthermostable NAD-dependent glutamate dehydrogenase from the archaeon *Pyrobaculum islandicum* and effects of denaturants and organic solvents. Appl Environ Microbiol 64:2152–2157

Lee YH, Nadaraia S, Gu D, Becker DF, Tanner JJ (2003) Structure of the proline dehydrogenase domain of the multifunctional PutA flavoprotein. Nat Struct Biol 10:109–114

Lee HS, Kang SG, Bae SS, Lim JK, Cho Y, Kim YJ, Jeon JH, Cha SS, Kim HT, Park CJ, Lee HW, Kim SI, Chun J, Colwell RR, Kim SJ, Lee JH (2008) The complete genome sequence of *Thermococcus onnurineus* NA1 reveals a mixed heterotrophic and carboxydotrophic metabolism. J Bacteriol 190:7491–7499

Lee HS, Bae SS, Kim MS, Kwon KK, Kang SG, Lee JH (2011) Complete genome sequence of *Pyrococcus* sp. strain NA2, isolated from a deep-sea hydrothermal vent area. J Bacteriol 193:3066–3067

Li WF, Zhou XX, Lu P (2005) Structural features of thermozymes. Biotechnol Adv 23:271–281

Lim LW, Mathews FS, Steenkamp DJ (1988) Identification of ADP in the iron–sulfur flavoprotein trimethylamine dehydrogenase. J Biol Chem 263:3075–3078

Maeder DL, Weiss RB, Dunn DM, Cherry JL, González JM, DiRuggiero J, Robb FT (1999) Divergence of the hyperthermophilic archaea *Pyrococcus furiosus* and *P. horikoshii* inferred from complete genomic sequences. Genetics 152:1299–1305

Mardanov AV, Ravin NV, Svetlitchnyi VA, Beletsky AV, Miroshnichenko ML, Bonch-Osmolovskaya EA, Skryabin KG (2009) Metabolic versatility and indigenous origin of the archaeon *Thermococcus sibiricus*, isolated from a Siberian oil reservoir, as revealed by genome analysis. Appl Environ Microbiol 75:4580–4588

Menzel R, Roth J (1981a) Purification of the putA gene product. A bifunctional membrane-bound protein from *Salmonella typhimurium* responsible for the two-step oxidation of proline to glutamate. J Biol Chem 256:9755–9761

Menzel R, Roth J (1981b) Enzymatic properties of the purified putA protein from *Salmonella typhimurium*. J Biol Chem 256:9762–9766

Monaghan PJ, Leys D, Scrutton NS (2007) Mechanistic aspects and redox properties of hyperthermophilic L-proline dehydrogenase from *Pyrococcus furiosus* related to dimethylglycine dehydrogenase/oxidase. FEBS J 274:2070–2087

Nisimoto Y, Wilson E, Heyl BL, Lambeth JD (1986) NADH dehydrogenase from bovine neutrophil membranes. Purification and properties. J Biol Chem 261:285–290

Ohshima T, Soda K (1989) Thermostable amino acid dehydrogenases: application and gene cloning. Trends Biotechnol 7:210–214

Sakuraba H, Takamatsu Y, Satomura T, Kawakami R, Ohshima T (2001) Purification, characterization, and application of a novel dye-linked L-proline dehydrogenase from a hyperthermophilic archaeon, *Thermococcus profundus*. Appl Environ Microbiol 67:1470–1475

Satomura T, Kawakami R, Sakuraba H, Ohshima T (2002) Dye-linked D-proline dehydrogenase from hyperthermophilic archaeon *Pyrobaculum islandicum* is a novel FAD-dependent amino acid dehydrogenase. J Biol Chem 277:12861–12867

Satomura T, Kawakami R, Sakuraba H, Ohshima T (2008) A novel flavin adenine dinucleotide (FAD) containing D-lactate dehydrogenase from the thermoacidophilic crenarchaeota *Sulfolobus tokodaii* strain 7: purification, characterization and expression in *Escherichia coli*. J Biosci Bioeng 106:16–21

Satomura T, Sakuraba H, Hara Y, Ohshima T (2010) Crystallization and preliminary X-ray analysis of a novel dye-linked L-proline dehydrogenase from the aerobic hyperthermophilic archaeon *Aeropyrum pernix*. Acta Crystallogr Sect F Struct Biol Cryst Commun 66:1508–1510

Satomura T, Zhang XD, Hara Y, Doi K, Sakuraba H, Ohshima T (2011) Characterization of a novel dye-linked L-proline dehydrogenase from an aerobic hyperthermophilic archaeon, *Pyrobaculum calidifontis*. Appl Microbiol Biotechnol 89:1075–1082

Scarpulla RC, Soffer RL (1978) Membrane-bound proline dehydrogenase from *Escherichia coli*. Solubilization, purification, and characterization. J Biol Chem 253:5997–6001

Srivastava D, Schuermann JP, White TA, Krishnan N, Sanyal N, Hura GL, Tan A, Henzl MT, Becker DF, Tanner JJ (2010) Crystal structure of the bifunctional proline utilization A flavoenzyme from *Bradyrhizobium japonicum*. Proc Natl Acad Sci USA 107:2878–2883

Tanner JJ (2008) Structural biology of proline catabolism. Amino Acids 35:719–730

Tsuge H, Kawakami R, Sakuraba H, Ago H, Miyano M, Aki K, Katunuma N, Ohshima T (2005) Crystal structure of a novel FAD-, FMN-, and ATP-containing L-proline dehydrogenase complex from *Pyrococcus horikoshii*. J Biol Chem 280:31045–31049

Vannier P, Marteinsson VT, Fridjonsson OH, Oger P, Jebbar M (2011) Complete genome sequence of the hyperthermophilic, piezophilic, heterotrophic, and carboxydotrophic archaeon *Thermococcus barophilus* MP. J Bacteriol 193:1481–1482

White TA, Krishnan N, Becker DF, Tanner JJ (2007) Structure and kinetics of monofunctional proline dehydrogenase from *Thermus thermophilus*. J Biol Chem 282:14316–14327

Zhang M, White TA, Schuermann JP, Baban BA, Becker DF, Tanner JJ (2004) Structures of the *Escherichia coli* PutA proline dehydrogenase domain in complex with competitive inhibitors. Biochemistry 43:12539–12548

Zheng H, Hirose Y, Kimura T, Suye S, Hori T, Katayama H, Arai J, Kawakami R, Ohshima T (2006) L-Proline sensor based on layer-by-layer immobilization of thermostable dye-linked L-proline dehydrogenase and polymerized mediator. Sci Technol Adv Mater 7:243–248

Zheng H, Lin L, Okezaki Y, Kawakami R, Sakuraba H, Ohshima T, Takagi K, Suye S (2010) Electrochemical behavior of dye-linked L-proline dehydrogenase on glassy carbon electrodes modified by multi-walled carbon nanotubes. Beilstein J Nanotechnol 1:135–141

Zivanovic Y, Armengaud J, Lagorce A, Leplat C, Guérin P, Dutertre M, Anthouard V, Forterre P, Wincker P, Confalonieri F (2009) Genome analysis and genome-wide proteomics of *Thermococcus gammatolerans*, the most radioresistant organism known amongst the Archaea. Genome Biol 10:R70